MOLEKUL
eISSN: 2503-0310

Articles
https://doi.org/10.20884/1.jm.2026.21.2.17616

A Combined Molecular Docking, Dynamics Simulation, and In Vitro Evaluation of Hydroxythioxanthones as Antidiabetic and Antioxidant Candidates

Faris Hermawan[1], Anita Dwi Puspitasari[2]*, Ririn Lispita Wulandari[2], Muhammad Eka Prastya[1], Minarti Minarti[1], Nik Nur Syazni Nik Mohamed Kamal[3], Hasna Marwa Annazwa[4], Sorta Dwi Margaretta Nababan[4]

[1]Research Center for Pharmaceutical Ingredients and Traditional Medicine, National Research and Innovation Agency (BRIN), Serpong, Tangerang Selatan 15354, Banten, Indonesia
[2]Faculty of Pharmacy, Universitas Wahid Hasyim, Semarang, Indonesia
[3]Department of Toxicology, Advanced Medical and Dental Institute, Universiti Sains Malaysia, Kepala Batas, Penang 13200, Malaysia
[4]Department of Chemistry, Faculty of Mathematics and Natural Sciences, Universitas Negeri Semarang, Jawa Tengah, Indonesia

*Corresponding author email: anita@unwahas.ac.id

Received August 27, 2025; **Accepted** June 08, 2026; **Available online** July 20, 2026

ABSTRACT. This research conducts a comprehensive investigation of hydroxythioxanthone derivatives through an integrated methodology that includes molecular docking, molecular dynamics (MD) simulations, and in vitro evaluations of antidiabetic and antioxidant activities. Molecular docking and MD simulations were performed to elucidate the binding interactions and dynamic stability of these compounds in complex with the α-glucosidase enzyme. The docking results indicated that the hydroxythioxanthone derivatives exhibited binding affinities ranging from −5.48 to −6.42 kcal/mol. In contrast, α-D-glucopyranose and quercetin demonstrated higher binding affinities of −6.99 and −7.01 kcal/mol, respectively. Subsequently, 100 ns MD simulations confirmed the stability of the ligand–protein complexes, as evidenced by consistently low values of root mean square deviation (RMSD), root mean square fluctuation (RMSF), and radius of gyration (Rg). The antidiabetic activity assay revealed that 4-chloro-1-hydroxythioxanthone (TX4) and 2,4-dichloro-1,3-dihydroxythioxanthone (TX5) exhibited strong inhibitory effects against α-glucosidase, with IC_{50} values of 78.35 and 91.97 μg/mL, respectively, whereas quercetin showed a lower IC_{50} value of 1.25 μg/mL. Furthermore, the antioxidant evaluation demonstrated that 2-chloro-1-hydroxythioxanthone (TX3) and 4-chloro-1-hydroxythioxanthone (TX4) possessed IC_{50} values of 87.48 and 17.72 μg/mL, respectively, while ascorbic acid served as the reference compound with an IC_{50} value of 9.15 μg/mL.

Keywords: antidiabetic, antioxidant, molecular docking, molecular dynamics, thioxanthone

INTRODUCTION

Diabetes mellitus is a chronic metabolic disorder distinguished by elevated blood glucose levels (Poznyak et al., 2020). The two primary forms of diabetes mellitus are insulin-dependent diabetes mellitus (IDDM), commonly referred to as type 1 diabetes, and non-insulin-dependent diabetes mellitus (NIDDM), known as type 2 diabetes. Both types share common characteristics, including postprandial hyperglycemia (PPHG) (Jadon et al., 2024). Type 2 diabetes mellitus (T2DM) is a chronic metabolic condition characterized by insulin resistance and elevated blood glucose levels. It affects more than 463 million individuals globally and represents a significant challenge for healthcare systems worldwide (Sun et al., 2022). Postprandial hyperglycemia serves as a significant contributor to complications associated with diabetes. This phenomenon is primarily governed by the enzymatic activities of α-amylase and α-glucosidase, which facilitate the conversion of complex carbohydrates into absorbable monosaccharides (Gong et al., 2020). Inhibition of these enzymes has emerged as a clinically validated strategy for managing T2DM, as evidenced by the widespread use of acarbose and miglitol (Dirir et al., 2022). However, the clinical application of these inhibitors is frequently limited by gastrointestinal adverse effects, including flatulence, abdominal distension, and diarrhea, resulting from the fermentation of undigested carbohydrates in the intestine. These limitations highlight the need for the development of novel therapeutic agents with improved pharmacological profiles (He et al., 2014).

α-Glucosidase is a critical enzymatic mediator in the terminal stage of carbohydrate digestion, catalyzing the hydrolysis of oligosaccharides into absorbable monosaccharides within the brush border membrane of the small intestinal epithelium. Inhibition

of this enzyme acts through a reversible, competitive mechanism whereby inhibitor molecules occupy the enzyme's active sites, thereby delaying monosaccharide release and attenuating postprandial glycemic excursions (Gul et al., 2024). Therapeutic modulation of α-glucosidase activity, in conjunction with enhanced glucose uptake in peripheral tissues, represents a well-established and clinically relevant strategy for maintaining glycemic homeostasis in individuals with type 2 diabetes mellitus (T2DM) (Khan et al., 2024).

Research on oxidative stress-related diseases has garnered significant attention due to its detrimental and severe impact on human health (Liguori et al., 2018). Numerous life-threatening conditions, including cancer, arthritis, cardiovascular diseases, and neurodegenerative disorders, are attributed to oxidative stress, which inflicts damage on human tissues and organs (Gutteridge & Halliwell, 2018). Reactive oxygen species (ROS) represent a class of chemical compounds produced during the metabolism of oxygen, and they significantly contribute to oxidative stress, which can damage lipids, proteins, and DNA (Juan et al., 2021). Furthermore, free radical ROS play a crucial role in the deposition of cholesterol and the development of atherosclerosis within blood vessels (Batty et al., 2022). Consequently, researchers are undertaking comprehensive efforts to prevent and neutralize these free radicals before their potentially harmful effects on cellular functions (Neha et al., 2019). The utilization of antioxidant compounds represents a fundamental and mechanistically straightforward approach for the neutralization of reactive oxygen species and other free radicals (Gulcin, 2020). A significant proportion of these agents are phenolic in nature, primarily due to their intrinsic capacity to donate hydrogen atoms and to stabilize unpaired electrons through resonance delocalization, thereby effectively interrupting oxidative chain reactions and preventing the onset of oxidative stress (Michalak, 2022).

Xanthone and its derivatives have been extensively reported to exhibit a wide spectrum of pharmacological activities, including anticancer (Hermawan et al., 2024), antimalarial (Hastuti et al., 2024), antioxidant (Gampa et al., 2022), and antidiabetic effects (Jovanović et al., 2024). Numerous studies have highlighted the potential of xanthone-based compounds as antidiabetic agents (Soares et al., 2022). In particular, xanthone derivatives bearing hydroxyl substituents have demonstrated inhibitory activity against α-glucosidase, with reported IC_{50} values of 7.08 and 13.4 μM. Furthermore, the incorporation of halogen substituents (e.g., F, Cl, Br, I) has also been associated with enhanced antidiabetic activity (Ke et al., 2024). Regarding antioxidant properties, 1,3,8-trihydroxyxanthone, 1,7-dihydroxyxanthone, and 1,5,6-trihydroxyxanthone exhibited IC_{50} values of 653, 349, and 524 μM, respectively (Fatmasari et al., 2022).

Numerous studies have reported the antidiabetic and antioxidant properties of hydroxyxanthone derivatives. However, investigations focused on thioxanthone derivatives, particularly those with hydroxyl, chloro, and bromo substituents, are limited. Addressing this research gap, the present study aims to evaluate the pharmacological potential of a series of substituted thioxanthone derivatives through molecular docking, molecular dynamics simulations, and in vitro assays. The compounds examined in this study include 1-hydroxythioxanthone (TX1), 1,3-dihydroxythioxanthone (TX2), 2-chloro-1-hydroxythioxanthone (TX3), 4-chloro-1-hydroxythioxanthone (TX4), 2,4-dichloro-1,3-dihydroxythioxanthone (TX5), and 2,4-dibromo-1,3-dihydroxythioxanthone (TX6). Their antidiabetic and antioxidant activities were assessed through α-glucosidase inhibition and 1,1-diphenyl-2-picrylhydrazyl (DPPH) radical scavenging assays.

EXPERIMENTAL SECTION

Materials

The thioxanthone derivatives employed in this study including 1-hydroxythioxanthone (TX1), 1,3-dihydroxythioxanthone (TX2), 2-chloro-1-hydroxythioxanthone (TX3), 4-chloro-1-hydroxythioxanthone (TX4), 2,4-dichloro-1,3-dihydroxythioxanthone (TX5), and 2,4-dibromo-1,3-dihydroxythioxanthone (TX6), were synthesized as previously reported (Hermawan et al., 2022, 2024). The chemical structure of hydroxythioxanthone derivatives (TX1-TX6) is shown in **Figure 1**. The in vitro assays were conducted using methanol, 2,2-diphenyl-1-picrylhydrazyl (DPPH), ascorbic acid, dimethyl sulfoxide (DMSO), phosphate buffer, α-glucosidase enzyme, and sodium bicarbonate.

Molecular Docking Study

The crystal structure of α-glucosidase complexed with α-D-glucopyranose (PDB ID : 3A4A) was retrieved from the Protein Data Bank (https://www.rcsb.org/pdb). Protein and native ligand structures were separated using UCSF Chimera, and the resulting coordinates were saved in PDB format (Meng et al., 2023). The molecular structures of the thioxanthone derivatives were constructed using Avogadro software and subsequently optimized using the ORCA quantum chemistry program, employing the DFT B3LYP functional with a 3-21G basis set (**Figure 1**) (Neese et al., 2020). The optimized geometries were then exported in .pdb format for use in docking procedures. Molecular docking and redocking simulations were performed using AutoDock4 with a grid box size of 30 × 30 × 30 Å centered at the active site. The coordinates of the central grid point were set at x = 21.240, y = −7.742, and z = 24.343 (Morris et al., 2009). The Lamarckian

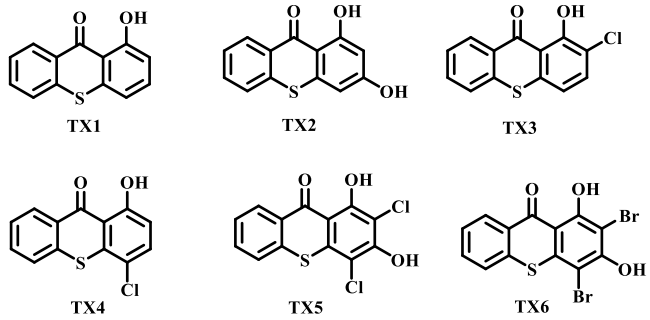

Figure 1. Chemical structure of hydroxythioxanthone derivatives (TX1-TX6)

Genetic Algorithm (LGA) was utilized for 50 independent docking runs. Among the generated docking conformations, the pose exhibiting the lowest binding energy was selected as the representative binding mode for subsequent analysis. Resulting docking poses and binding interactions were analyzed and visualized using Discovery Studio Visualizer (DSV) 2019 (Biovia, 2019).

Molecular Dynamics Simulation

Molecular dynamics (MD) simulations for the hydroxythioxanthone derivatives were carried out using the GROMACS 2023 simulation package, and the topology of the target protein was generated based on the CHARMM36 all-atom force field parameters (Huang & MacKerell, 2013). For the ligand molecules, topology and force field parameters were derived using the CHARMM General Force Field (CGenFF) via the automated topology generation interface (Hess et al., 2008), ensuring compatibility with the CHARMM-based simulation environment. Each protein–ligand complex was embedded within a cubic simulation box and solvated using approximately 11,508 water molecules. To maintain electrostatic neutrality, an appropriate number of sodium ions was added. Periodic boundary conditions (PBC) were applied in all directions to emulate an infinite system. Prior to molecular dynamics simulations, energy minimization was carried out using the steepest descent algorithm for a maximum of 50,000 steps, terminating when the maximum force decreased below 1000 kJ/mol/nm to remove unfavorable steric interactions. The system was subsequently equilibrated in two sequential phases of 100 ps each. The first phase involved NVT equilibration at 300 K, during which position restraints were applied to the protein–ligand complex, and temperature was regulated using the velocity-rescale (V-rescale) thermostat (Bernetti & Bussi, 2020). This was followed by NPT equilibration at 1 bar, where pressure was controlled using the coordinate-rescale (C-rescale) barostat while maintaining the temperature at 300 K (Bernetti & Bussi, 2020). Long-range electrostatic interactions were treated using the Particle Mesh Ewald (PME) method (George et al., 2022). Subsequently, production molecular dynamics simulations were performed for 100 ns under NPT conditions at 300 K and 1 bar. The structural stability and dynamic behavior of the protein–ligand complexes were evaluated by analyzing root mean square deviation (RMSD), root mean square fluctuation (RMSF), and radius of gyration (Rg) throughout the simulation trajectories.

Antidiabetic Activity

The antidiabetic potential of the compounds was evaluated via an α-glucosidase inhibition assay. Briefly, 5 μL of the test compound dissolved in DMSO was combined with 45 μL of phosphate buffer, followed by the sequential addition of 25 μL of the α-glucosidase enzyme and 25 μL of the substrate solution. The reaction mixture was incubated at room temperature for 15 minutes to allow enzymatic activity. Subsequently, 100 μL of 0.2 M sodium bicarbonate was added to terminate the reaction. The absorbance of the resulting solution was measured at a wavelength of 400 nm using a microplate reader. The percentage of enzyme inhibition was determined by calculating the absorbance values of the sample (S1), background sample (S0), blank (B1), and background blank (B0) using the following formula:

$$\%\text{Inhibition} = \frac{[(A_{b1} - A_{b0}) - (A_{S1} - A_{S0})]}{(A_{b1} - A_{b0})}\ x\ 100\%$$

A range of sample concentrations (200–6.25 ppm) was tested, and all experiments were performed in triplicate (n = 3). The IC_{50} values were calculated from the inhibition curves using linear regression analysis with Microsoft Excel and are presented as mean ± standard deviation (SD).

Antioxidant Activity

The antioxidant activity of hydroxythioxanthone derivatives (TX1–TX6) was evaluated using the 2,2-diphenyl-1-picrylhydrazyl (DPPH) radical scavenging assay. Each compound was dissolved in methanol to obtain a concentration range of 0.39–50 µg mL^{-1}. An aliquot of each solution was mixed with a 1000 µg mL^{-1} DPPH methanolic solution and incubated under dark conditions for 30 minutes to prevent photo-degradation. L-ascorbic acid was employed as a positive control. The absorbance was measured at 517 nm using a microplate reader (EPOC, USA), and the percentage of radical inhibition was subsequently calculated using the standard formula.

$$\%\text{Inhibition} = \{1\text{-}\frac{A_{sample} - A_{control}}{A_{blank} - A_{control}}\}\ x\ 100\%$$

The 50% inhibitory concentration (IC_{50}) was calculated using linear regression analysis of the inhibition values obtained from experiments performed in triplicate (n = 3). The IC_{50} values were determined using Microsoft Excel and are presented as mean ± standard deviation (SD).

RESULTS AND DISCUSSION

Molecular Docking Study

Molecular docking represents a structure-based computational strategy employed to predict the binding conformation and interaction profile of small molecules within the active site of a target receptor, providing insights into binding affinities and potential intermolecular interactions (Agu et al., 2023). The docking protocol is considered reliable when the RMSD between the top-ranked docked pose and the crystallographic ligand conformation is ≤ 2 Å, indicating that the predicted binding orientation closely reproduces the experimentally observed structure (Jiang & Rizzo, 2015). In this study, redocking of α-D-glucopyranose yielded an RMSD value of 0.81 Å, confirming that the docking parameters were appropriate and reliable for the docking simulations (**Figure 2**).

The docking analysis revealed that the thioxanthone derivatives (TX1–TX6) exhibited binding energies ranging from –5.48 to –6.42 kcal/mol, whereas the reference compounds α-D-glucopyranose and quercetin demonstrated binding energies of –6.99 and –7.01 kcal/mol, respectively (**Table 1**). The hydroxythioxanthone derivatives exhibited higher binding energy values compared to α-D-glucopyranose and quercetin, suggesting comparatively weaker inhibitory potential. In molecular docking analysis, lower binding energy reflects a more favorable and stable interaction between the ligand and the target protein, indicating greater binding affinity and complex stability (Hari, 2019).

All thioxanthone derivatives were found to interact with the α-glucosidase enzyme through various non-covalent interactions, including hydrogen bonding, van der Waals forces, π–sulfur, π–anion, π–cation, and π–alkyl interactions, as illustrated in **Figure 2**. The native ligand, α-D-glucopyranose, formed hydrogen bond interactions with several key residues within the active site, including Asp69, His112, Arg213, Asp215, Glu277, His351, Ser352, and Arg442, whereas the reference inhibitor Quercetin interacted with residues Arg213, Asp215, Glu277, Gln279, and Glu411. Notably, several thioxanthone derivatives shared common interacting residues with these reference ligands. For instance, TX1 formed hydrogen bond interactions with Arg213, a residue also involved in the binding of both α-D-glucopyranose and quercetin. TX2 interacted with Asp69 and Asp215, which are also observed in the interactions of α-D-glucopyranose and quercetin, respectively. Furthermore, TX3, TX4, TX5, and TX6 exhibited hydrogen bond interactions with Glu411, a residue also involved in quercetin binding, while TX4 and TX6 additionally interacted with Gln279. The presence of these shared interacting residues suggests that the thioxanthone derivatives may occupy a similar binding region within the catalytic pocket of α-glucosidase, thereby supporting a potentially comparable binding mode and inhibitory mechanism relative to the reference ligands.

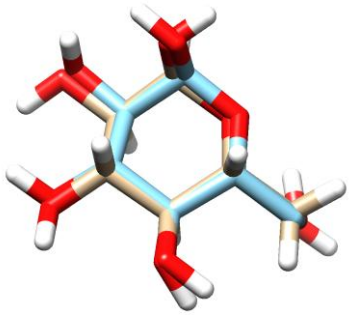

Figure 2. Overlay of α-D-glucopyranose structures before docking (white) and after docking (blue)

Table 1. Molecular docking results of hydroxythioxanthone derivatives

Compound	Binding energy (kcal/mol)	Hydrogen bond
TX1	-5.48	Arg213, Glu227
TX2	-6.55	Asp69, Asp215, His315
TX3	-5.97	Glu411
TX4	-5.89	Gln279, Glu411
TX5	-6.08	Arg315, Glu411
TX6	-6.42	Gln279, Glu411
α-D-glucopyranose	-6.99	Asp69, His112, Arg213, Asp215, Glu277, His351, Asp352, Arg442

Quercetin	-7.01	Arg213, Asp215, Glu277, Gln279, Glu411

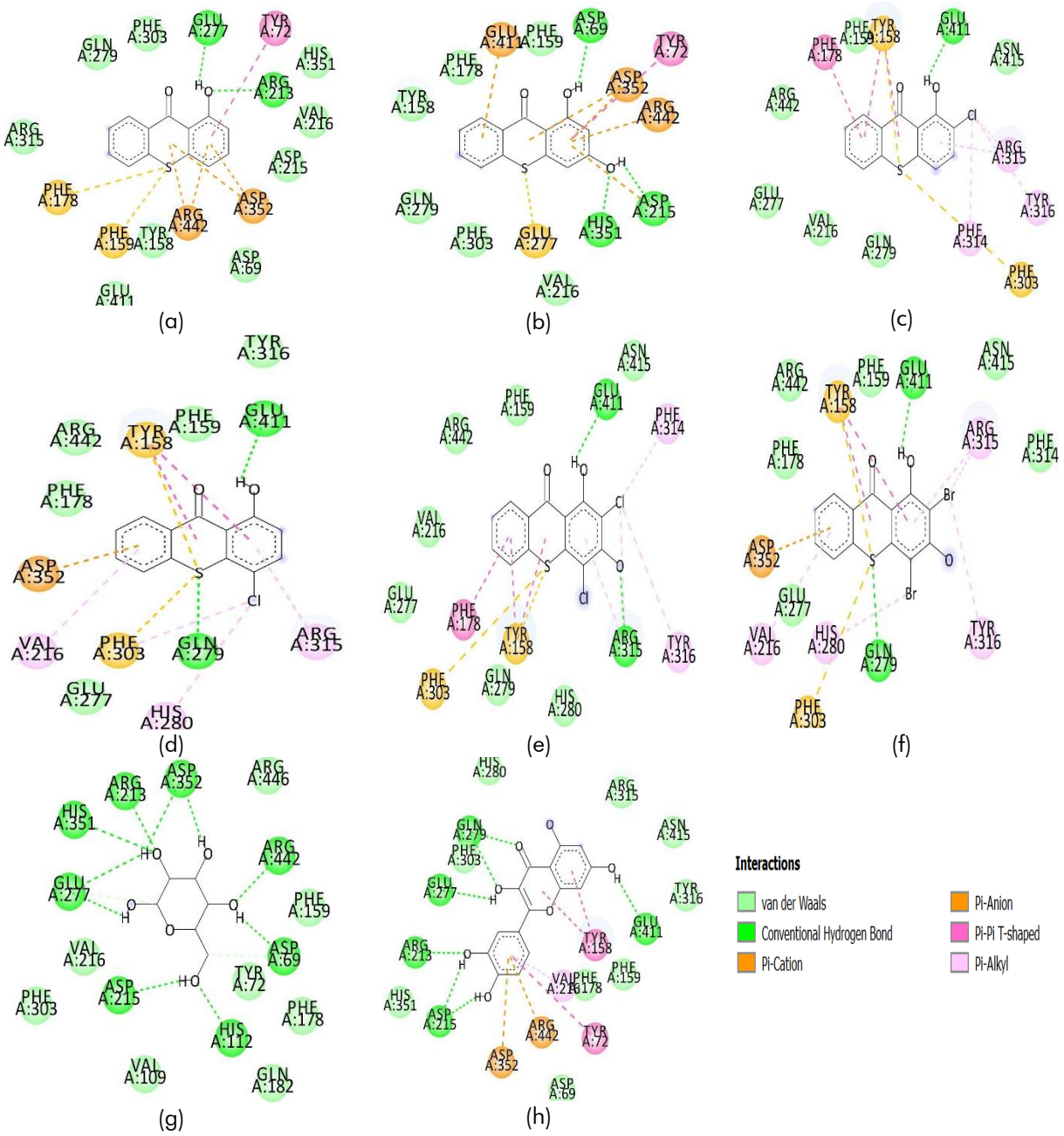

Figure 3. The interactions (**a**) **TX1**, (**b**) **TX2**, (**c**) **TX3**, (**d**) **TX4**, (**e**) **TX5**, (**f**) **TX6**, (**g**) α-D-glucopyranose and (**h**) Quercetin

Molecular Dynamics Simulation

An in-depth characterization of the protein–ligand complexes was conducted via molecular dynamics (MD) simulations over a 100-nanosecond timescale to elucidate their structural integrity and dynamic conformational behavior. The RMSD parameter was utilized to quantitatively assess temporal deviations in the protein backbone structure, calculated by comparing atomic positions relative to the initial reference conformation throughout the simulation trajectory. The structural stability of the protein during the simulation trajectory can be inferred from the magnitude of conformational deviations, wherein lower RMSD values and minimal fluctuations are indicative of enhanced structural robustness and equilibrium maintenance (Aier et al., 2016). As depicted in **Figure 4a**, the RMSD values of all ligands remained below 2.0 Å throughout the simulation period. These consistently low RMSD values suggest that the ligands maintained stable binding within the active site, exhibiting minimal conformational fluctuations or rotational displacement. The RMSD profiles of the ligands relative to the protein backbone ranged from approximately 2 to 16 Å during the 100 ns molecular dynamics simulation (**Figure 4**). The initial increase in RMSD likely reflects conformational

adjustments of the ligands within the α-glucosidase binding pocket. After approximately 30 ns, the RMSD values became relatively stable with moderate fluctuations, indicating that the systems reached dynamic equilibrium. These fluctuations may be attributed to the flexibility of the thioxanthone derivatives and the large binding cavity of α-glucosidase, suggesting that the complexes remained dynamically stable during the simulation. Additionally, α-D-glucopyranose exhibited the lowest and most consistent RMSD throughout the 100 ns simulation time. Quercetin reached RMSD stabilization after approximately 30 ns of molecular dynamics simulation, indicating a stable interaction with the target. Compounds TX2 to TX6 had relatively consistent RMSD values. In contrast, compound TX1 exhibited the highest RMSD values, although it eventually achieved convergence beyond 30 ns. These results indicate that TX1 exhibits comparatively lower structural stability in complex with α-D-glucopyranose, Quercetin, and other compounds, suggesting a less stable binding interaction.

Root mean square fluctuation (RMSF) analysis provides residue-level insights into the dynamic flexibility of the protein throughout the molecular dynamics trajectory. Higher RMSF values indicate increased flexibility of specific residues, whereas lower values reflect structural rigidity and stability (Bagewadi et al., 2023). As illustrated in **Figure 5a**, the RMSF profiles of all simulated complexes display generally similar fluctuation patterns, indicating that ligand binding does not substantially alter the global dynamic behavior of the α-glucosidase enzyme. Notable fluctuations were observed in several regions, particularly around residues 140–160, 220–240, 290–310, and 410–430, which correspond to loop regions typically associated with increased structural flexibility in proteins. In contrast, residues located within the predicted ligand-binding pocket identified from the molecular docking analysis exhibited relatively low RMSF values, suggesting that ligand interactions contribute to maintaining local structural stability during the simulation. Although minor variations in residue flexibility were observed among complexes containing hydroxythioxanthone derivatives, α-D-glucopyranose, and quercetin, these differences were primarily localized in peripheral regions and did not significantly affect the structural stability of the binding pocket. Overall, the RMSF results indicate that ligand binding induces only limited localized flexibility while preserving the structural integrity of the α-glucosidase active site throughout the simulation.

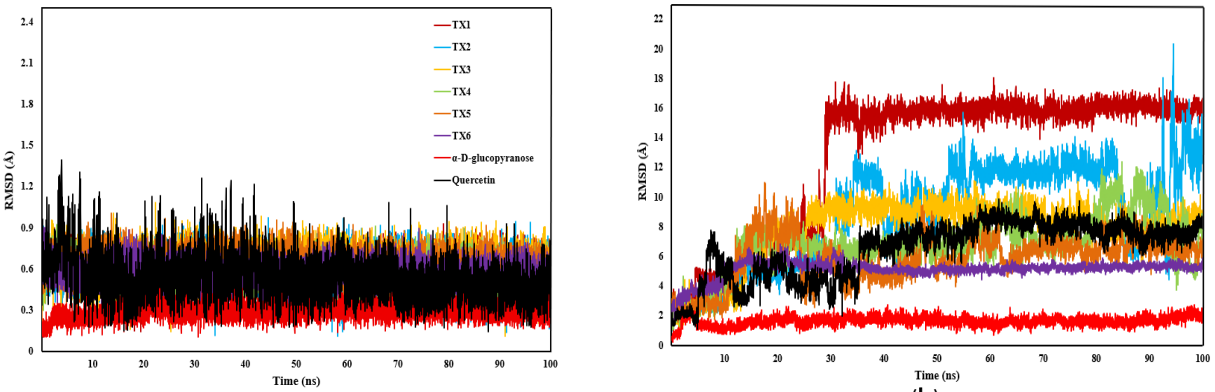

Figure 4. RMSD graphs of (**a**) ligands and (**b**) ligand-protein backbone complexes

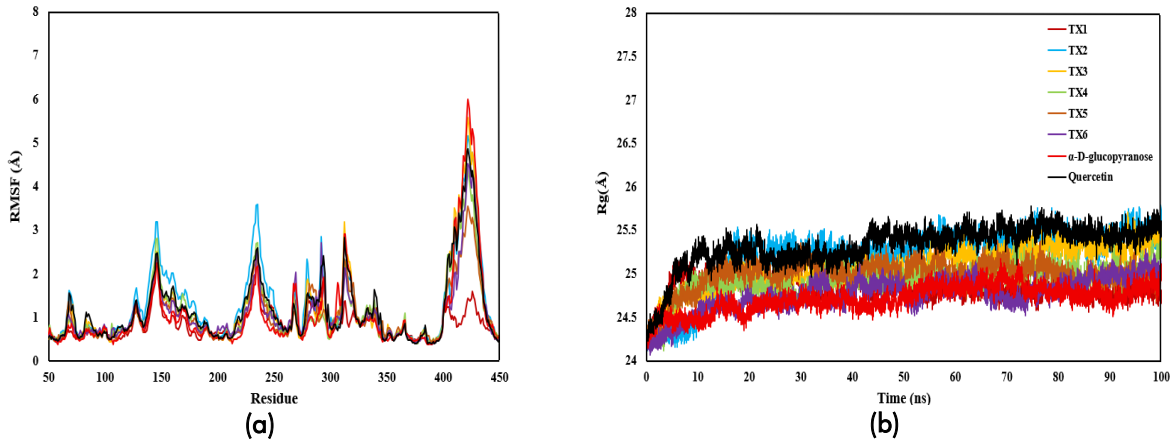

Figure 5. (**a**) RMSF and (**b**) Radius of gyration of compounds TX1-6, α-D-glucopyranose, and Quercetin

The radius of gyration (Rg) serves as an indicator of the overall compactness of a protein structure, defined as the root mean square distance of the constituent atoms from the molecule's center of mass. Lower Rg values are typically associated with more compact and globular conformations, while higher values reflect an extended and potentially less stable structural arrangement (Bagewadi et al., 2023). As depicted in **Figure 5b**, the Rg profiles of all ligand–protein complexes remained relatively consistent throughout the simulation, indicating that ligand binding either promoted or preserved the structural integrity of the protein. Notably, the α-D-glucopyranose complex exhibited the lowest Rg values, suggesting a more compact and stabilizing interaction with the α-glucosidase enzyme.

Antidiabetic Activity

The antidiabetic activity of six thioxanthone derivatives, including 1-hydroxythioxanthone (TX1), 1,3-dihydroxythioxanthone (TX2), 2-chloro-1-hydroxythioxanthone (TX3), 4-chloro-1-hydroxythioxanthone (TX4), 2,4-dichloro-1,3-dihydroxythioxanthone (TX5), and 2,5-dibromo-1,3-dihydroxythioxanthone (TX6) was evaluated through α-glucosidase inhibition assays. Quercetin, a compound previously reported to inhibit α-glucosidase, was used as the positive control. Antidiabetic activity was categorized based on IC_{50} values, with compounds exhibiting $IC_{50} \leq 50$ µg/mL considered very strong, 50–100 µg/mL as strong, 101–150 µg/mL as moderate, and ≥ 151 µg/mL as weak inhibitors (Culas et al., 2021). The antidiabetic activity data are presented in **Table 2**. Compounds TX2, and TX3 demonstrated IC_{50} values exceeding 151 µg/mL and are therefore categorized as weak inhibitors of α-glucosidase. Additionally, compounds TX1 and TX6 demonstrated an IC_{50} value of 119.63 and 108.01 μg/mL, thereby placing them within the category of moderate antidiabetic activity. These findings follow the molecular docking results, where compound TX1 exhibited the highest binding energy. Consistently, molecular dynamics simulations revealed that TX1 displayed the highest RMSD value, suggesting relatively weaker and less stable interactions with the target protein. Subsequent analysis revealed that compounds TX2 and TX3 exhibited increased RMSD values. Notably, TX2 demonstrated pronounced fluctuations in RMSD after 80 ns of molecular dynamics simulation, indicating potential structural instability within the protein-ligand complex.

In contrast, TX4 and TX5 demonstrated considerable inhibitory activity against α-glucosidase, with IC_{50} values of 78.35 and 91.97 μg/mL, respectively, and were thus categorized as strong α-glucosidase inhibitors. These findings imply that the incorporation of chloro substituents into the hydroxythioxanthone framework (TX4 and TX5) contributes to an enhancement of antidiabetic efficacy. Moreover, quercetin, used as the positive control, exhibited the lowest IC_{50} value (1.25 μg/mL), indicating strong inhibitory activity against α-glucosidase. Quercetin is widely recognized as a potent natural α-glucosidase inhibitor and is frequently employed as a reference compound in in vitro inhibition assays (Koh et al., 2022; Şöhretoğlu et al., 2018), thereby providing a useful benchmark for evaluating the antidiabetic potential of the tested compounds

Antioxidant Activity

The antioxidant potential of hydroxythioxanthone derivatives (TX1–TX6) was evaluated using the 2,2-diphenyl-1-picrylhydrazyl (DPPH) radical scavenging assay, a widely employed and standardized method for assessing free radical inhibition. Based on IC_{50} values, antioxidant activity was categorized as follows: highly active (<50 µg/mL), active (50–100 µg/mL), moderate (101–250 µg/mL), mild (251–500 µg/mL), and inactive (>500 µg/mL) (Rahman & Huda, 2021). The antioxidant properties of the hydroxythioxanthone derivatives were evaluated in terms of their IC_{50}, as presented in **Table 3**. All compounds demonstrated higher IC_{50} values relative to L-ascorbic acid, the reference standard, indicating comparatively lower radical scavenging efficiency. Compounds TX1 and TX2 exhibited comparatively high IC_{50} values, 327.62 and 283.90 $\mu g\ mL^{-1}$, respectively, and were therefore categorized as displaying only mild activity. By contrast, TX5 and TX6 yielded IC_{50} values of 158.83 and 195.20 $\mu g\ mL^{-1}$, corresponding to moderate activity. Compound TX3 recorded an IC_{50} of 87.48 $\mu g\ mL^{-1}$, classifying it as active in terms of antioxidant capacity. Notably, among all derivatives examined, TX4 achieved the lowest IC_{50} value, 17.72 $\mu g\ mL^{-1}$, indicative of very strong antioxidant efficacy.

Table 2. The IC_{50} values of thioxanthone derivatives as α-glucosidase inhibitor

Compound	IC_{50} (μg/mL)	SD
TX1	119.63	± 10.75
TX2	283.09	-
TX3	173.09	± 32.94
TX4	78.35	± 28.78
TX5	91.97	± 19.45
TX6	108.01	± 8.58
Quercetin	1.25	± 0.17

Table 3. In vitro antioxidant activity of hydroxythioxanthone derivatives

Compound	IC_{50} (μg/mL)	SD
TX1	327.62	± 43.25
TX2	283.90	± 98.09
TX3	87.48	± 14.81
TX4	17.72	± 3.79
TX5	158.83	± 25.63
TX6	158.78	± 6.63
Ascorbic acid	9.15	± 0.57

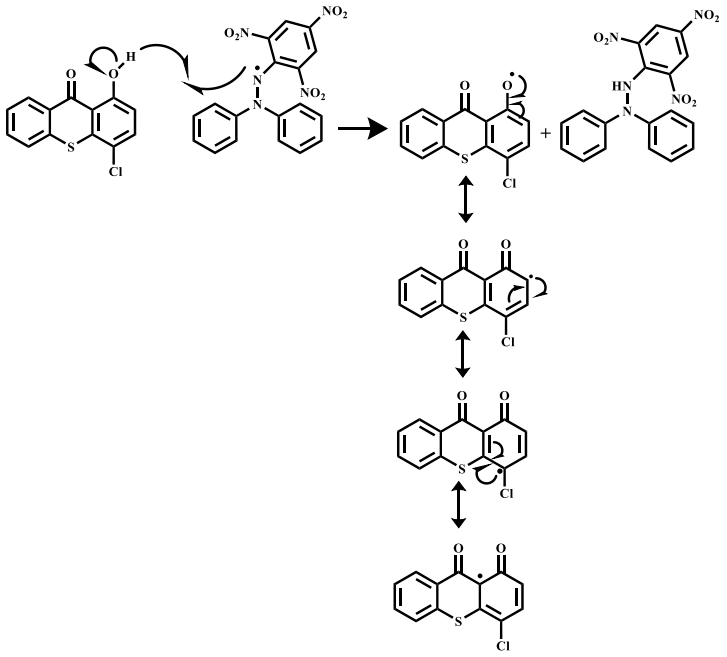

Figure 6. The plausible reaction of DPPH free radical with compound TX4

An increased number of hydroxyl groups on the xanthone framework has been associated with reduced antioxidant activity, likely due to the formation of stronger intramolecular hydrogen bonds among the hydroxyl moieties (Fatmasari et al., 2022). Although compounds TX2, TX5, and TX6 possess a higher number of hydroxyl substituents relative to TX3 and TX4, they exhibited comparatively lower antioxidant activity. This effect is likely due to the close positioning of the hydroxyl groups within the molecular structure, which limits the accessibility of DPPH free radicals to these functional groups, thus diminishing antioxidant activity (França et al., 2013). A plausible hydrogen atom transfer (HAT) mechanism for the reaction of DPPH free radicals with compound TX4 is illustrated in **Figure 6**, adapted from literature-reported mechanisms for hydroxyxanthones (Fatmasari et al., 2022).

CONCLUSIONS

The molecular docking analysis demonstrated that hydroxythioxanthone derivatives (**TX1**–**TX6**) exhibited binding affinities ranging from −5.48 to −6.42 kcal/mol. In comparison, α-D-glucopyranose and quercetin displayed stronger binding energies of −6.99 and −7.01 kcal/mol, respectively. Subsequent molecular dynamics simulations over 100 ns revealed that the root mean square deviation (RMSD) values of all ligand–protein complexes remained below 2.0 Å, indicating that all compounds maintained stable interactions within the active site, with minimal conformational fluctuations or rotational displacement. In vitro antidiabetic evaluation indicated that TX4 and TX5 exhibited relatively low IC_{50} values of 78.35 and 91.97 μg/mL, respectively, whereas quercetin showed a significantly lower IC_{50} of 1.25 μg/mL. In terms of antioxidant activity, TX3 and TX4 demonstrated IC_{50} values of 87.48 and 17.72 μg/mL, respectively, while ascorbic acid exhibited an IC_{50} of 9.15 μg/mL. Taken together, TX4 exhibited the most favorable bioactivity profiles in both antidiabetic and antioxidant assays, suggesting its considerable potential as a promising candidate for the development of novel multifunctional therapeutic agents.

ACKNOWLEDGEMENTS

We are grateful to Universitas Wahid Hasyim for the financial support for our research via the International Research Scheme with contract number 7/LPPM-UWH/Research-DIPA/2025.

REFERENCES

Agu, P. C., Afiukwa, C. A., Orji, O. U., Ezeh, E. M., Ofoke, I. H., Ogbu, C. O., Ugwuja, E. I., & Aja, P. M. (2023). Molecular docking as a tool for the discovery of molecular targets of nutraceuticals in diseases management. *Scientific Reports*, *13*(1), 13398. https://doi.org/10.1038/s41598-023-40160-2

Aier, I., Varadwaj, P. K., & Raj, U. (2016). Structural insights into conformational stability of both wild-type and mutant EZH2 receptor. *Scientific Reports*, *6*, 34984. https://doi.org/10.1038/srep34984

Bagewadi, Z. K., Yunus Khan, T. M., Gangadharappa, B., Kamalapurkar, A., Mohamed Shamsudeen, S., & Yaraguppi, D. A. (2023). Molecular dynamics and simulation analysis against superoxide dismutase (SOD) target of *Micrococcus luteus* with secondary metabolites from *Bacillus licheniformis* recognized by genome mining approach. *Saudi Journal of Biological Sciences*, *30*(9), 103753. https://doi.org/https://doi.org/10.1016/j.sjbs.2023.103753

Batty, M., Bennett, M. R., & Yu, E. (2022). The Role of Oxidative Stress in Atherosclerosis. *Cells*, *11*(23). https://doi.org/10.3390/cells 11233843

Biovia, D. S. (2019). Discovery Studio Visualizer. *San Diego*.

Culas, S., Marapana, R., Palangasinghe, I., & Liyanage, A. (2021). Development of liquid-based tea and its antidiabetic effect. *Journal of Chemistry*, *2021*, 1–6. https://doi.org/10.1155/2021/8863936

Dirir, A. M., Daou, M., Yousef, A. F., & Yousef, L. F. (2022). A review of alpha-glucosidase inhibitors from plants as potential candidates for the treatment of type-2 diabetes. *Phytochemistry Reviews : Proceedings of the Phytochemical Society of Europe*, *21*(4), 1049–1079. https://doi.org/10.1007/s11101-021-09773-1

Fatmasari, N., Kurniawan, Y. S., Jumina, J., Anwar, C., Priastomo, Y., Pranowo, H. D., Zulkarnain, A. K., & Sholikhah, E. N. (2022). Synthesis and in vitro assay of hydroxyxanthones as antioxidant and anticancer agents. *Scientific Reports*, *12*(1), 1535. https://doi.org/10.1038/s41598-022-05573-5

França, H. S., Rocha, L., Fernande, C. P., Ruiz, A. L. T. G., & de Carvalho, J. E. (2013). Antiproliferative activity of the hexanic extract and phloroglucinols from Hypericum brasiliense. *Revista Brasileira de Farmacognosia*, *23*(5), 844–847. https://doi.org/https://doi.org/10.1590/S0102-695X2013000500018

Gampa, M., Padmaja, P., Khalivulla, S. I., & Reddy, P. N. (2022). Synthesis and antimicrobial and antioxidant activities of 1,2,3-triazole-tethered xanthone derivatives. *Russian Journal of Organic Chemistry*, *58*(6), 872–877. https://doi.org/10.1134/S1070428022060173

Gong, L., Feng, D., Wang, T., Ren, Y., Liu, Y., & Wang, J. (2020). Inhibitors of α-amylase and α-glucosidase: Potential linkage for whole cereal foods on prevention of hyperglycemia. *Food Science & Nutrition*, *8*(12), 6320–6337. https://doi.org/10.1002/fsn3.1987

Gul, S., Jan, F., Alam, A., Shakoor, A., Khan, A., AlAsmari, A. F., Alasmari, F., Khan, M., & Bo, L. (2024). Synthesis, molecular docking and DFT analysis of novel bis-Schiff base derivatives with thiobarbituric acid for α-glucosidase inhibition assessment. *Scientific Reports*, *14*(1), 3419. https://doi.org/10.1038/s41598-024-54021-z

Gulcin, İ. (2020). Antioxidants and antioxidant methods: an updated overview. *Archives of Toxicology*, *94*(3), 651–715. https://doi.org/10.1007/s00204-020-02689-3

Gutteridge, J. M. C., & Halliwell, B. (2018). Mini-Review: Oxidative stress, redox stress or redox success? *Biochemical and Biophysical Research Communications*, *502*(2), 183–186. https://doi.org/10.1016/j.bbrc.2018.05.045

Hari, S. (2019). In silico molecular docking and ADME/T analysis of plant compounds against IL17A and IL18 targets in gouty arthritis. *Journal of Applied Pharmaceutical Science*, *9*(7), 018–026. https://doi.org/10.7324/JAPS.2019.90703

Hastuti, L. P., Hermawan, F., Iresha, M. R., Ernawati, T., & Firdayani. (2024). In-silico studies of hydroxyxanthone derivatives as potential pfDHFR and pfDHODH inhibitor by molecular docking, molecular dynamics simulation, MM-PBSA calculation and pharmacokinetics prediction. *Informatics in Medicine Unlocked*, *47*, 101485. https://doi.org/https://doi.org/10.1016/j.imu.2024.101485

He, K., Shi, J.-C., & Mao, X.-M. (2014). Safety and efficacy of acarbose in the treatment of diabetes in Chinese patients. *Therapeutics and Clinical Risk Management*, *10*, 505–511. https://doi.org/10.2147/TCRM.S50362

Hermawan, F., Jumina, J., Pranowo, H., Sholikhah, E., Ernawati, T., & Azminah, A. (2024). In silico approach for design, synthesis and biological evaluation of tioxanthone derivatives as potential anticancer agents. *ChemistrySelect*, *9*. https://doi.org/10.1002/slct.202304014

Hermawan, F., Jumina, J., Pranowo, H., Sholikhah, E., & Iresha, M. (2022). Molecular docking approach for design and synthesis of thioxanthone derivatives as anticancer agents. *ChemistrySelect*, *7*. https://doi.org/10.1002/slct.202203076

Hess, B., Kutzner, C., van der Spoel, D., & Lindahl, E.

(2008). GROMACS 4: Algorithms for highly efficient, load-balanced, and scalable molecular simulation. *Journal of Chemical Theory and Computation*, *4*(3), 435–447. https://doi.org/10.1021/ct700301q

Huang, J., & MacKerell, A. D. J. (2013). CHARMM36 all-atom additive protein force field: validation based on comparison to NMR data. *Journal of Computational Chemistry*, *34*(25), 2135–2145. https://doi.org/10.1002/jcc.23354

Jadon, A. S., Kaushik, M. P., Anitha, K., Bhatt, S., Bhadauriya, P., & Sharma, M. (2024). *Chapter 1 - Types of diabetes mellitus, mechanism of insulin resistance and associated complications* (P. Tripathi, R. P. Tripathi, & M. P. B. T.-B. I. of D. and A. C. Kaushik (eds.); pp. 1–18). Academic Press. https://doi.org/https://doi.org/10.1016/B978-0-443-13195-0.00001-6

Jiang, L., & Rizzo, R. C. (2015). Pharmacophore-based similarity scoring for DOCK. *The Journal of Physical Chemistry. B*, *119*(3), 1083–1102. https://doi.org/10.1021/jp506555w

Jovanović, J. A., Krstić-Milošević, D., Vinterhalter, B., Dinić, S., Grdović, N., Uskoković, A., Rajić, J., Đorđević, M., Sarić, A., Vidaković, M., & Mihailović, M. (2024). Evaluation of the antidiabetic potential of xanthone-rich extracts from *Gentiana dinarica* and gentiana utriculosa. In *International Journal of Molecular Sciences* (Vol. 25, Issue 16). https://doi.org/10.3390/ijms25169066

Juan, C. A., Pérez de la Lastra, J. M., Plou, F. J., & Pérez-Lebeña, E. (2021). The chemistry of reactive oxygen species (ROS) revisited: outlining their role in biological macromolecules (DNA, lipids and proteins) and induced pathologies. *International Journal of Molecular Sciences*, *22*(9). https://doi.org/10.3390/ijms22094642

Ke, Y., Xu, Q., Hu, J., Zhang, J., Chen, S., Liu, Z., Peng, S., Zhang, C., Chen, Z., & Chen, H. (2024). Xanthones with multiple roles against diabetes: their synthesis, structure-activity relationship, and mechanism studies. *Drug Development Research*, *85*(2), e22170. https://doi.org/10.1002/ddr.22170

Khan, M., Ahad, G., Alam, A., Ullah, S., Khan, A., Kanwal, Salar, U., Wadood, A., Ajmal, A., Khan, K. M., Perveen, S., Uddin, J., & Al-Harrasi, A. (2024). Synthesis of new bis(dimethylamino)benzophenone hydrazone for diabetic management: In-vitro and in-silico approach. *Heliyon*, *10*(1), e23323. https://doi.org/10.1016/j.heliyon.2023.e23323

Koh, Y. Q., Sin, Y. A. D., Rong, H. J., Chua, T. H. S., Ho, S.-H. S., & Ho, H. K. (2022). Evaluation of anthoxanthins and their actions on digestive enzyme inhibition when used independently and in combination. *Heliyon*, *8*(8), e10131. https://doi.org/10.1016/j.heliyon.2022.e10131

Meng, E. C., Goddard, T. D., Pettersen, E. F., Couch, G. S., Pearson, Z. J., Morris, J. H., & Ferrin, T. E. (2023). UCSF ChimeraX: Tools for structure building and analysis. *Protein Science : A Publication of the Protein Society*, *32*(11), e4792. https://doi.org/10.1002/pro.4792

Michalak, M. (2022). Plant-derived antioxidants: significance in skin health and the ageing process. *International Journal of Molecular Sciences*, *23*(2). https://doi.org/10.3390/ijms23020585

Neese, F., Wennmohs, F., Becker, U., & Riplinger, C. (2020). The ORCA quantum chemistry program package. *The Journal of Chemical Physics*, *152*, 224108. https://doi.org/10.1063/5.0004608

Neha, K., Haider, M. R., Pathak, A., & Yar, M. S. (2019). Medicinal prospects of antioxidants: A review. *European Journal of Medicinal Chemistry*, *178*, 687–704. https://doi.org/10.1016/j.ejmech.2019.06.010

Poznyak, A., Grechko, A. V, Poggio, P., Myasoedova, V. A., Alfieri, V., & Orekhov, A. N. (2020). The Diabetes mellitus-atherosclerosis connection: the role of lipid and glucose metabolism and chronic inflammation. *International Journal of Molecular Sciences*, *21*(5). https://doi.org/10.3390/ijms21051835

Rahman, M., & Huda, M. (2021). Exploration of phytochemical, antioxidant and anti-inflammatory efficacy of the ethnomedicinal uses of ten orchids of Bangladesh. *Advancement in Medicinal Plant Research*, *9*(2), 30–39.

Soares, J. X., Loureiro, D. R. P., Dias, A. L., Reis, S., Pinto, M. M. M., & Afonso, C. M. M. (2022). Bioactive marine xanthones: A Review. *Marine Drugs*, *20*(1). https://doi.org/10.3390/md20010058

Şöhretoğlu, D., Sari, S., Barut, B., & Özel, A. (2018). Discovery of potent α-glucosidase inhibitor flavonols: Insights into mechanism of action through inhibition kinetics and docking simulations. *Bioorganic Chemistry*, *79*, 257–264. https://doi.org/10.1016/j.bioorg.2018.05.010

Sun, H., Saeedi, P., Karuranga, S., Pinkepank, M., Ogurtsova, K., Duncan, B. B., Stein, C., Basit, A., Chan, J. C. N., Mbanya, J. C., Pavkov, M. E., Ramachandaran, A., Wild, S. H., James, S., Herman, W. H., Zhang, P., Bommer, C., Kuo, S., Boyko, E. J., & Magliano, D. J. (2022). IDF Diabetes Atlas: Global, regional and country-level diabetes prevalence estimates for 2021 and projections for 2045. *Diabetes Research and Clinical Practice*, *183*, 109119. https://doi.org/10.1016/j.diabres.2021.109119

Jiang, L., & Rizzo, R. C. (2014). Pharmacophore-based similarity scoring for DOCK. *The Journal*

of Physical Chemistry B, 119(3), 1083–1102. https://doi.org/10.1021/jp506555w

Bussi, G., Donadio, D., & Parrinello, M. (2007). Canonical sampling through velocity rescaling. *The Journal of Chemical Physics, 126*(1), 014101. https://doi.org/10.1063/1.2408420

Darden, T., York, D., & Pedersen, L. (1993). Particle mesh Ewald: An N·log(N) method for Ewald sums in large systems. *The Journal of Chemical Physics, 98*(12), 10089–10092. https://doi.org/10.1063/1.464397

He, K., Shi, J.-C., & Mao, X.-M. (2014). Safety and efficacy of acarbose in the treatment of diabetes in Chinese patients. *Therapeutics and Clinical Risk Management, 10*, 505–511. https://doi.org/10.2147/TCRM.S50350